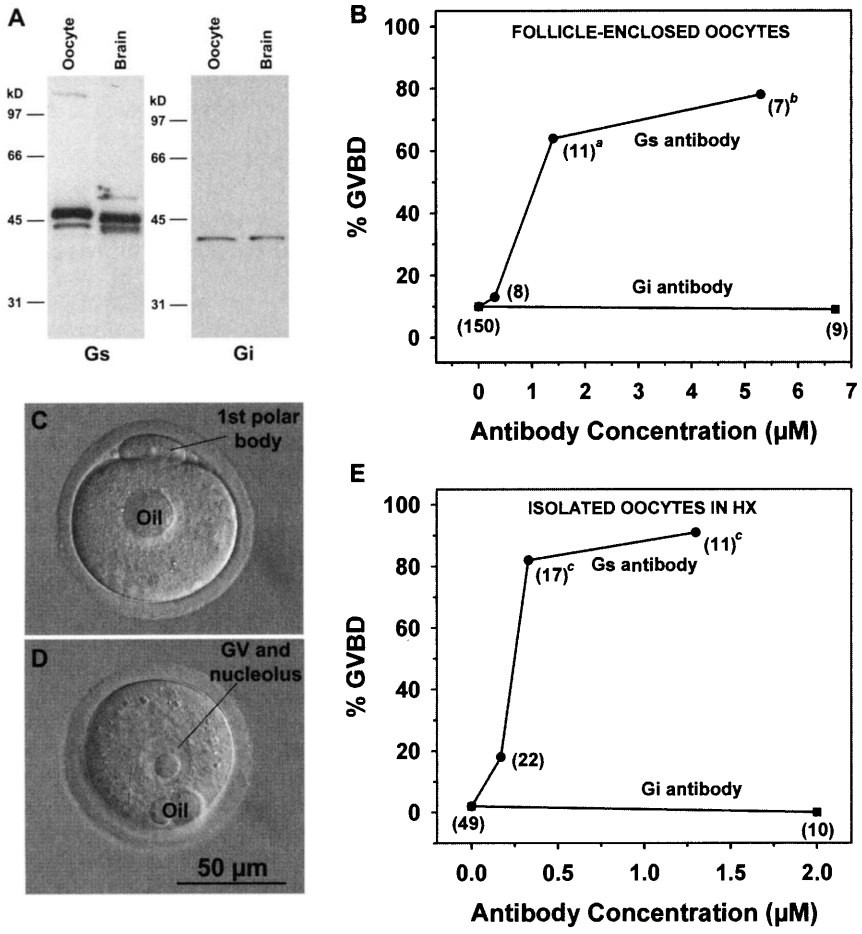

Fig. 2. Injection of an antibody against G_s causes oocyte maturation. (**A**) Immunoblots showing G_s and G_i protein in mouse oocytes and brain probed with the same antibodies used for microinjection. Total protein per lane = 4, 2.5, 5, and 5 μg for lanes 1 to 4, respectively. (**B**) Follicle-enclosed oocytes were injected with an antibody against G_s or with a control antibody against G_i; the graph shows antibody concentrations in the cytoplasm (the 0 μM point describes uninjected oocytes from follicles processed in parallel). Three hours later, the oocytes were removed from their follicles and scored for the presence or absence of a nucleus (% GVBD). (**C**) Formation of a polar body by an oocyte injected with the G_s antibody (1.3 μM). The oocyte was removed from the follicle 3 hours after injection, at which time it had undergone GVBD; it was photographed 20 hours later. (**D**) Control oocyte injected with the G_i antibody (6.7 μM) and removed from the follicle 3 hours later, at which time the GV was intact. (**E**) Isolated oocytes were injected with antibodies against G_s or G_i, incubated in the presence of 4 mM hypoxanthine (Hx), and scored for GVBD 3 hours later. For (B) and (E), numbers in parentheses indicate the number of oocytes injected with each antibody concentration, and superscript letters indicate the statistical significance of the results compared with G_i antibody-injected controls (*a*, $P < 0.03$; *b*, $P < 0.01$; *c*, $P < 0.001$; Fisher's exact test) (*4*).

of signaling molecules from the follicle that maintain meiotic arrest in the oocyte as well as the mechanism by which luteinizing hormone causes the resumption of meiosis.

References and Notes

1. J. J. Eppig, in *The Ovary*, E. Y. Adashi, P. C. K. Leung, Eds. (Raven Press, New York, 1993), pp. 185–208.
2. E. Anderson, D. F. Albertini, *J. Cell Biol.* **71**, 680 (1976).
3. S. M. Downs, R. Buccione, J. J. Eppig, *J. Exp. Zool.* **262**, 391 (1992).
4. Supplementary materials and methods are available on *Science* Online.
5. D. P. Kiehart, *Methods Cell Biol.* **25**, 13 (1982).
6. W. F. Simonds, P. K. Goldsmith, J. Codina, C. G. Unson, A. M. Spiegel, *Proc. Natl. Acad. Sci. U.S.A.* **86**, 7809 (1989).
7. W. F. Simonds, P. K. Goldsmith, C. J. Woodard, C. G. Unson, A. M. Spiegel, *FEBS Lett.* **249**, 189 (1989).
8. C. J. Gallo, A. R. Hand, T. L. Z. Jones, L. A. Jaffe, *J. Cell Biol.* **130**, 275 (1995).
9. J. D. Robishaw, M. D. Smigel, A. G. Gilman, *J. Biol. Chem.* **261**, 9587 (1986).
10. R. Bruzzone, T. W. White, D. L. Paul, *Eur. J. Biochem.* **238**, 1 (1996).
11. T. Iiri, P. Herzmark, J. M. Nakamoto, C. Van Dop, H. R. Bourne, *Nature* **371**, 164 (1994).
12. P. Chidiac, T. E. Hebert, M. Valiquette, M. Dennis, M. Bouvier, *Mol. Pharmacol.* **45**, 490 (1994).
13. R. A. F. de Ligt, A. P. Kourounakis, A. P. Ijzerman, *Br. J. Pharmacol.* **130**, 1 (2000).
14. J. J. Eppig, P. F. Ward-Bailey, D. L. Coleman, *Biol. Reprod.* **33**, 1041 (1985).
15. T. G. Baker, in *Reproduction in Mammals, Book 1*, C. R. Austin, R. V. Short, Eds. (Cambridge Univ. Press, Cambridge, 1982), pp. 17–45.

16. We thank A. Spiegel for providing antibodies; J. Eppig and D. Myles for helpful advice; and A. Cowan, R. Kalinowski, T. Kishimoto, D. Kline, M. Pixley, L. Ross, L. Runft, M. Terasaki, J. Zimmerberg, and the anonymous reviewers for critical reading of the manuscript. Supported by a postdoctoral fellowship from the Lalor Foundation to L.M.M. and by grants from the National Institutes of Health and the Human Frontiers Science Program to L.A.J.

Supporting Online Material
www.sciencemag.org/cgi/content/full/297/5585/1343/DC1
Materials and Methods
SOM Text
Figs. S1 and S2
References

14 May 2002; accepted 15 July 2002

Distinct Modes of Signal Recognition Particle Interaction with the Ribosome

Martin R. Pool,[1]* Joachim Stumm,[1] Tudor A. Fulga,[2] Irmgard Sinning,[2]† Bernhard Dobberstein[1]

Signal recognition particle (SRP), together with its receptor (SR), mediates the targeting of ribosome-nascent chain complexes to the endoplasmic reticulum. Using protein cross-linking, we detected distinct modes in the binding of SRP to the ribosome. During signal peptide recognition, SRP54 is positioned at the exit site close to ribosomal proteins L23a and L35. When SRP54 contacts SR, SRP54 is rearranged such that it is no longer close to L23a. This repositioning may allow the translocon to dock with the ribosome, leading to insertion of the signal peptide into the translocation channel.

Secretory proteins are synthesized with an NH_2-terminal hydrophobic signal peptide, which is recognized by the SRP as it emerges from the ribosome (*1*, *2*). SRP targets the ribosome, together with the associated nascent chain, to the endoplasmic reticulum (ER) via

interaction with its receptor (SR), a heterodimeric ER membrane protein (*1*, *3*). SR coordinates the release of SRP from the ribosome–nascent chain complex (RNC) and the insertion of the nascent chain into the translocation channel formed by the Sec61 complex (*4*–*6*). During targeting, SRP induces a transient retardation of translation (elongation arrest), which prolongs the time window during which the RNC is competent for translocation (*7*, *8*). SRP is composed of a 7S RNA and six proteins with masses of 9, 14, 19, 54, 68, and 72 kD (*1*, *2*). The 54-kD subunit (SRP54) recognizes the signal peptide (*9*, *10*) and interacts with SR, whereas the SRP9 and -14 proteins are required for elongation arrest (*7*, *8*). Targeting is regulated by three guanosine triphosphatases (GTPases), namely, SRP54 and the two subunits of the SRP receptor (SRα and SRβ) (*11*–*13*). A ribosomal component stimulates GTP binding to SRP54, activating it for interaction with SR (*14*). To identify which ribosomal proteins SRP54 interacts with and to understand how the interaction of SRP54 with the ribosome changes during the targeting reaction, we used cross-linking to probe the molecular environment of SRP54 at defined stages of targeting.

RNCs were formed by translating a messenger RNA (mRNA) that lacks a stop codon so that the nascent chain is not released from the ribosome. The RNCs were generated from an mRNA encoding the first 86 residues of the secretory protein preprolactin (RNC_{pPL86}) (*15*). As a control, we also used an mRNA encoding a mutant pPL86 ($RNC_{pPL86\text{-}mut}$) that is unable to bind SRP54 with high affinity and hence cannot promote translocation (*16*, *17*). After the addition of purified canine SRP or purified SRP54, cross-linking was induced with disuccinimidyl suberate (DSS). Treatment of SRP alone with DSS did not lead to the formation of any SRP54 cross-link products (*18*). In the presence of wheat germ RNC_{pPL86} and SRP, DSS treatment resulted in the formation of three major cross-link species sized 61, 66, and 71 kD, corresponding to cross-link adducts of 7, 12, and 17 kD, respectively (Fig. 1A, lane 1). When RNC_{pPL86} produced in rabbit reticulocytes was used, a similar cross-link pattern was observed (lane 2), indicating a similar type of interaction independent of the source of ribosomes. The 7-kD cross-link partner corresponds to the nascent chain, as this cross-link product could be immunoprecipitated with antisera to prolactin (PL) (Fig. 2A). In the lanes where no SRP was added, cross-reactivity to residual wheat germ and rabbit SRP54 was observed (lanes 4 to 5); however, no cross-link products were visible. Cross-linking performed with $RNC_{pPL86\text{-}mut}$ produced a cross-linking profile identical to that with RNC_{pPL86} (lane 3). Cross-links between SRP54 and 12- and 17-kD proteins were also observed with SRP54 bound to ribosomes lacking a nascent chain (Fig. 1B), though the cross-link pattern was less well defined. When cross-linking was performed using radiolabeled SRP54 bound to RNC_{pPL86}, cross-linking to proteins of 7, 12, and 17 kD was observed (Fig. 1C). In contrast, cross-linking with $RNC_{pPL86\text{-}mut}$ gave a markedly different cross-link pattern. No cross-link product was formed between SRP54 and either the nascent chain or the 12-kD protein. The major cross-link product was formed with a 14-kD protein, which was not observed with the wild-type signal peptide. The cross-link product formed with the 17-kD adduct was still present, though reduced.

To determine whether the 12- and 17-kD proteins are core components of the ribosome and to identify the ribosomal subunit from which the proteins are derived, cross-linked RNC_{pPL86}-SRP complexes were treated with puromycin and a high concentration of salt to dissociate the ribosomes into 40S and 60S subunits. The subunits were then separated on a sucrose gradient and the fractions were analyzed by immunoblotting (Fig. 1C). The 12- and 17-kD cross-link adducts comigrated with the 60S subunit, indicating that they are core ribosomal proteins. The majority of the non–cross-linked SRP54 and nascent chain cross-link product localized to the top of the gradient as free SRP and in the 40S fractions. The presence of these two species in the 40S-containing fraction suggests an interaction of SRP with this subunit, probably mediated through components other than SRP54.

To identify the 12- and 17-kD cross-link partners, we raised antibodies to candidate proteins of the large subunit with corresponding sizes; these included L23a, L35, L30, and L37a (fig. S1, A and B). To test whether the antibod-

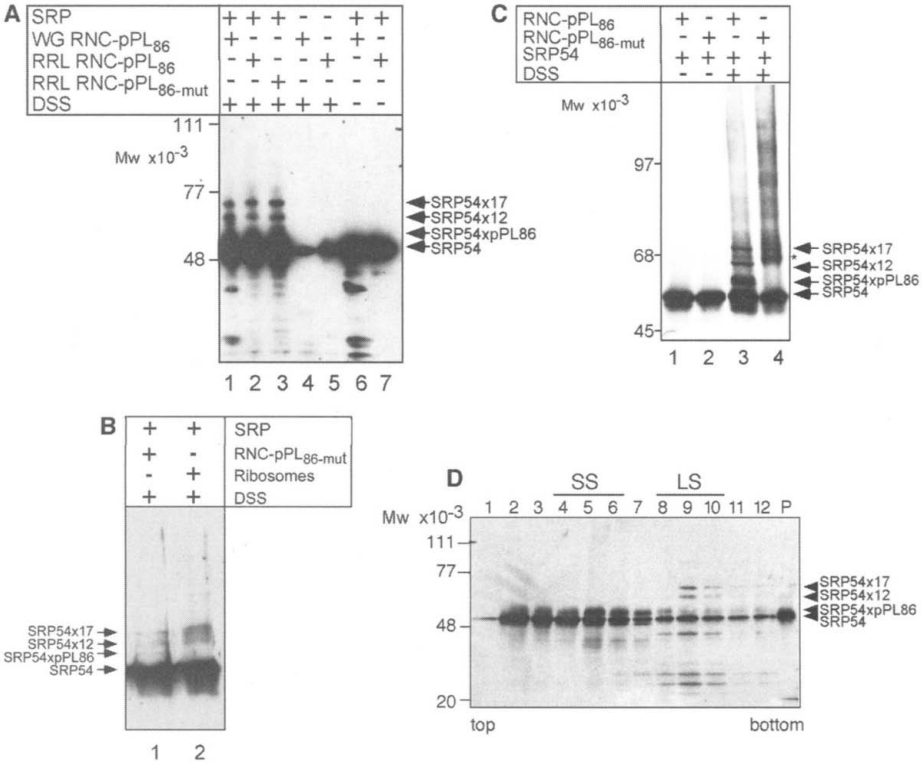

Fig. 1. Cross-linking of SRP54 to ribosomal components. (**A**) Purified canine SRP and RNC-pPL_{86} or RNC-$pPL_{86\text{-}mut}$, produced from wheat germ (WG) or rabbit reticulocytes (RRL), were treated, either alone or in combination, with the cross-linking reagent DSS (40 μM), as indicated. Cross-link products were visualized by SDS–polyacrylamide gel electrophoresis (SDS-PAGE) and immunoblotting with antibodies to SRP54. The cross-link adducts, together with their sizes, are indicated. (**B**) SRP was cross-linked (as described above) to either RNC-$pPL_{86\text{-}mut}$ or to nonprogrammed ribosomes, both derived from wheat germ. (**C**) Purified, radiolabeled SRP54 bound to wheat germ RNC-pPL_{86} or RNC-$pPL_{86\text{-}mut}$ was cross-linked with DSS and the reactions were analyzed by SDS-PAGE and phosphorimaging. The major cross-link product formed in the presence of RNC-$pPL_{86\text{-}mut}$ is indicated (*). (**D**) SRP was cross-linked to reticulocyte RNC-pPL_{86} with DSS. The ribosomes were then split into 40S and 60S subunits by treatment with puromycin and high salt, and the subunits separated by sucrose density gradient centrifugation. SRP54 cross-link products were detected by SDS-PAGE and immunoblotting. The positions of the large (LS) and small (SS) ribosomal subunits were deduced from the characteristic A254nm profile of the ribosomal RNAs (rRNAs).

[1]Zentrum für Molekulare Biologie der Universität Heidelberg (ZMBH), D-69120 Heidelberg, Germany. [2]Structural Biology Programme, European Molecular Biology Laboratory (EMBL), D-69117 Heidelberg, Germany.

*To whom correspondence should be addressed. E-mail: mrp@zmbh.uni-heidelberg.de

†Present address: Biochemiezentrum der Universität Heidelberg (BZH), D-69120 Heidelberg, Germany.

ies recognized the 12- or 17-kD proteins cross-linked to SRP54, radiolabeled SRP54 was cross-linked to RNC_{pPL86}, and then immunoprecipitation was carried out under denaturing conditions (Fig. 2A). Antibodies to SRP54 precipitated SRP54 and all the major cross-link products (lane 2). The 7-kD cross-link product was precipitated with PL antiserum (lane 3). The L23a antibodies precipitated the 17-kD crosslink, but not in the presence of the peptide antigen (lane 4). No SRP54 cross-link products were precipitated with the corresponding preimmune serum (lane 5). This indicates that the 17-kD adduct is L23a. The L23a antibodies also precipitated a 34-kD adduct, which could represent the cross-linking of L23a to another ribosomal protein. This was tested by treating ribosomes with DSS and then analyzing the proteins by Western blotting with L23a antibodies (Fig. 2B). L23a can indeed be cross-linked to another ribosomal protein to yield a 34-kD cross-link species. The homolog of L23a, L23, can be cross-linked to L29 in *E. coli* ribosomes (*19*), and these two proteins are closely positioned in the *Haloarcula marismortuii* 50S crystal structure (*20*). Therefore, we tested if the L23a cross-link partner was L35, the eukaryotic homolog of L29. Western blotting with L35 antibodies also revealed a 34-kD cross-link product that precisely comigrated with the L23a cross-link product. Thus, as in the 70S ribosome, L23a and L35 are closely positioned in the 60S subunit.

On the basis of the size and location of L35, the ability of L35 antibodies to precipitate the 12-kD cross-link adduct was tested (Fig. 2C). L35 antibodies specifically precipitated the 12-kD cross-link adduct (lane 3), but not in the presence of the peptide antigen (lane 4) nor with preimmune serum (lane 5). Antibodies against L30 and L37a did not precipitate any of the cross-link products (lanes 7 and 8), confirming that the 60S subunits were denatured before immunoprecipitation.

At the ER membrane, the RNC-SRP complex binds to SR via the interaction of SRP54 with SRα. GTP binding to both SRP54 and SRα leads to the formation of a stable "docked complex," which is necessary (*21*) but not sufficient (*6*) to promote release of the signal peptide from SRP. Release of the signal-peptide requires rearrangements in SR induced by the translocon (*6*, *22*).

In the absence of SR, SRP54 could be cross-linked to the same set of RNC proteins in the presence of either guanosine diphosphate (GDP) or the nonhydrolyzable GTP analog 5′-guanylylimidodiphosphate (GppNHp) (Fig. 3A, lanes 2 and 3). In the presence of SR and GDP, no major changes in the cross-link profile were observed (lane 4). When SR was present with GppNHp, cross-linking to the nascent chain and L35 persisted and was slightly enhanced (lane 5). In contrast, cross-linking to L23a was no longer detectable. Furthermore, additional cross-link products of ~180 kD that contain SRα were observed (Fig. 3B, lanes 4 and 5). When we performed cross-linking with GppNHp and a mutant SRP receptor that lacks the GTPase domain of SRα (*22*), no reduction in cross-linking to L23a was observed, nor were any additional SRP54 cross-link products formed (lane 6). Therefore, an intact SRα GTPase domain is required for both these events.

We also tested a minimal SRP, composed of radiolabeled SRP54 and the bacterial 4.5S RNA, which is functional in translocation (*16*). Cross-linking with RNC_{pPL86}-SRP54/4.5S RNA complexes yielded similar results to those obtained with the complete SRP (Fig. 3B, fig. S2). Treatment with DSS in the presence of SR and GppNHp but not GDP also led to the formation of the SRα cross-

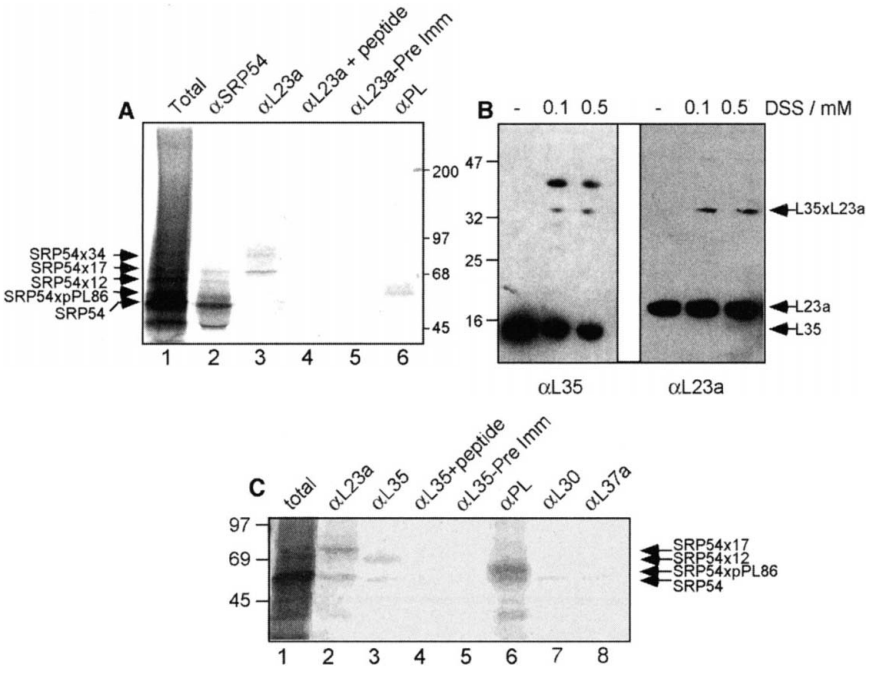

Fig. 2. Identification of SRP54 ribosomal cross-link partners. (**A**) Radiolabeled SRP54 was bound to $RNC\text{-}pPL_{86}$ and then treated with DSS. Immunoprecipitation was then performed under denaturing conditions with antibodies to SRP54, PL, L23a immune, and L23a preimmune (Pre-Imm). Where indicated, the L23a peptide antigen was also present during the immunoprecipitation. (**B**) Purified wheat germ ribosomes (3 pmol) were treated with DSS at the indicated concentrations and then were analyzed by SDS-PAGE and immunoblotting with antibodies to L23a and L35. (**C**) Cross-linking and denaturing immunoprecipitation was performed as in (A) but with antibodies to L23a, L35, L35-Pre-Imm, PL, L30, and L37a. Where indicated, L35 peptide antigen was present.

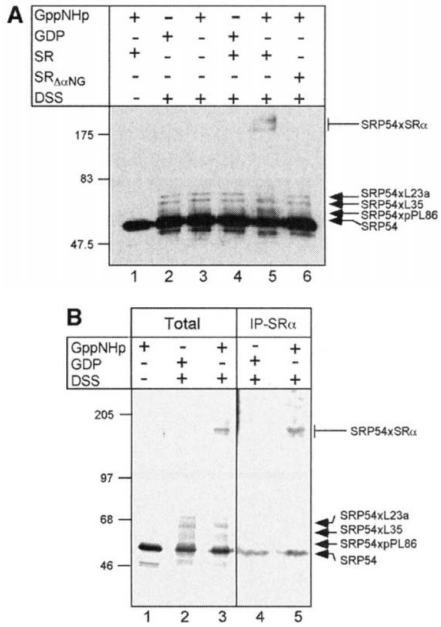

Fig. 3. Cross-linking of SRP54 to ribosomal proteins in the presence of SR. (**A**) Purified $RNC\text{-}pPL_{86}$-SRP complexes, prepared cotranslationally in reticulocyte lysate, were incubated either alone, with recombinant SR (0.25 μM) (*22*), or with recombinant SR, which lacks the SRα GTPase domain ($SR_{\Delta\alpha NG}$, 0.25 μM), in the presence of GDP (0.2 mM) or GppNHp (0.2 mM). Cross-linking was then induced with DSS. Reactions were analyzed by SDS-PAGE and immunoblotting. (**B**) $RNC\text{-}pPL_{86}$ complexes prepared in reticulocyte lysate were incubated with radiolabeled SRP54/4.5S RNA together with GDP (0.2 mM) or GppNHp (0.2 mM) and SR (0.25 μM), as indicated. Cross-linking was induced with DSS. Where indicated, the reactions were immunoprecipitated with SRα antibodies under denaturing conditions. Reactions were analyzed by SDS-PAGE and phosphorimaging. The 180-kD cross-link products are immunoprecipitated with SRα antibodies. These cross-link complexes appear to migrate anomalously, as the theoretical size of an SRP54 × SRα species is 125 kD.

link products (Fig. 3B). However, the reduction in cross-linking to L23a was not as pronounced as that observed with the intact SRP. This may be either because the minimal SRP interacts less efficiently with SR than the whole SRP or because other components of SRP facilitate the displacement of SRP54 by SR.

We have characterized the changing interaction of SRP54 with ribosomal proteins L23a and L35 during binding of SRP to the signal peptide and after contact of SRP with SR. The x-ray crystal structure of the archaeal 50S subunit (*20*, *23*) shows that the homologs of L23a and L35, L23 and L29, respectively, are surface-exposed and located close together on the ribosome near the site where the nascent chain emerges from the exit channel. A model derived from a cryo–electron microscopy (cryo-EM) reconstruction of the yeast 80S ribosome indicates that the homologs of L23a and L35 are also positioned at the exit site (*24*) (Fig. 4, A and B). This location of SRP54 is consistent with the fact that SRP54 can contact the signal peptide shortly after it emerges from the ribosome (*25*). Whole SRP can also bind to ribosomes in the absence of a nascent chain containing a signal peptide. In this case, SRP54 is also close to L23a and L35 at the exit site, consistent with SRP's function in scanning the ribosome for the presence of signal peptides (*26*). In contrast, cross-linking experiments using SRP54 alone revealed that, in the absence of the rest of the particle, SRP54 is only positioned close to L23a and L35 in the presence of a functional signal peptide. In the presence of a nonfunctional signal peptide, SRP54 is only close to L23a. A similar distinction was also found for GTP binding to SRP54 (*14*): When present in SRP, GTP binding was independent of a functional signal peptide. In contrast, binding of GTP to SRP54 alone depended on the presence of a functional signal peptide. Because GTP binding correlates with proximity of SRP54 to L35, it is tempting to speculate that it is the contact to this protein that triggers GTP binding and priming of SRP. A similar priming step in the activation of bacterial SRP (*Ffh*) has also been reported (*27*).

Contact of SRP with SR triggers further GTP binding to SRP54 and SRα (*21*), resulting in a tight interaction between the two molecules. Concomitantly, SRP54 is repositioned on the ribosome such that it is no longer in proximity to L23a (Fig. 4B). In the absence of the translocon, interaction with L35 persists and release of the signal-peptide does not occur, consistent with previous observations (*6*, *22*).

Reconstructions of ribosome-translocon complexes with the use of cryo-EM indicate that the ring-shaped Sec61p complex also binds to the ribosome at the exit site (*28*–*30*). Furthermore, the yeast homologs of L23a and L35 form a major contact with the Sec61p complex (*30*). This suggests that Sec61p and SRP54 bind to the ribosome in a mutually exclusive manner, which would explain the observation that SRP blocks direct binding of RNCs to Sec61p (*31*). This block in binding of the RNC-SRP complex to Sec61p can be relieved by SR and GTP. These conditions cause a repositioning of SRP54 relative to L23a and L35, suggesting a mechanism by which SR induces changes in SRP binding to the ribosome and permits access of Sec61p to the ribosome, such that the signal peptide can be efficiently transferred from SRP to the translocation complex.

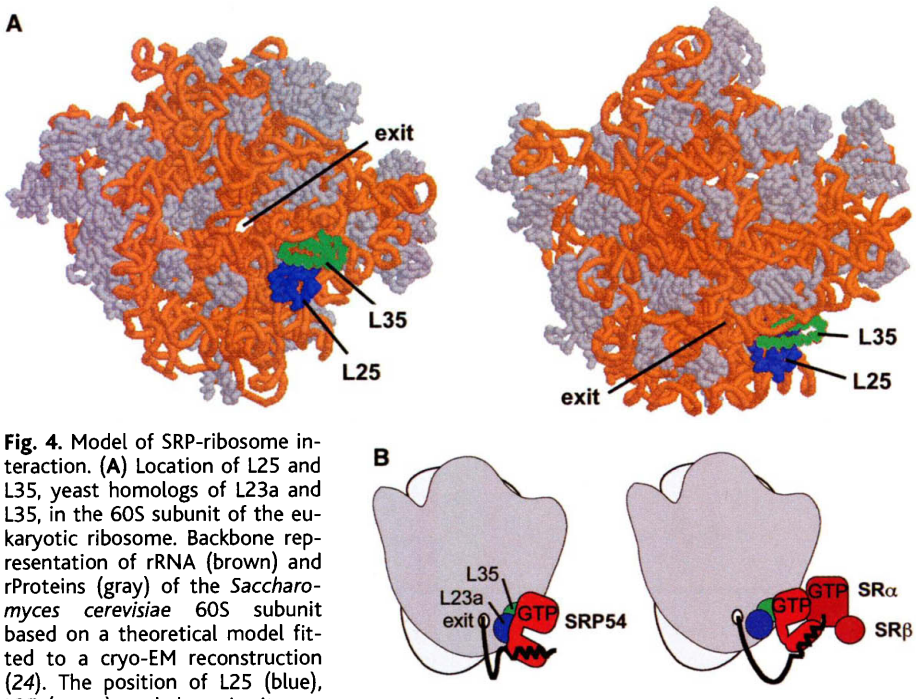

Fig. 4. Model of SRP-ribosome interaction. (**A**) Location of L25 and L35, yeast homologs of L23a and L35, in the 60S subunit of the eukaryotic ribosome. Backbone representation of rRNA (brown) and rProteins (gray) of the *Saccharomyces cerevisiae* 60S subunit based on a theoretical model fitted to a cryo-EM reconstruction (*24*). The position of L25 (blue), L35 (green), and the exit site are indicated. Left, viewed from the bottom of the subunit looking down the polypeptide channel. (Right) Crown view of the solvent-exposed face. (**B**) When SRP is bound to the ribosome, SRP54 is located at the exit site close to ribosomal proteins L23a and L35, where it can bind the signal peptide. Upon contact of SR, SRP54 is rearranged such that it is still bound to the signal peptide and L35 but is distal to L23a.

References and Notes

1. P. Walter, A. E. Johnson, *Annu. Rev. Cell Biol.* **10**, 87 (1994).
2. R. J. Keenan, D. M. Freymann, R. M. Stroud, P. Walter, *Annu. Rev. Biochem.* **70**, 755 (2001).
3. R. Gilmore, G. Blobel, P. Walter, *J. Cell Biol.* **95**, 463 (1982).
4. T. Rapoport, B. Jungnickel, U. Kutay, *Annu. Rev. Biochem.* **65**, 271 (1996).
5. A. E. Johnson, M. A. van Waes, *Annu. Rev. Cell Dev. Biol.* **16**, 799 (1999).
6. W. Song, D. Raden, E. C. Mandon, R. Gilmore, *Cell* **100**, 333 (2000).
7. V. Siegel, P. Walter, *J. Cell Biol.* **100**, 1913 (1985).
8. N. Mason, L. F. Ciufo, J. D. Brown, *EMBO J.* **19**, 4164 (2000).
9. T. V. Kurzchalia *et al.*, *Nature* **320**, 634 (1986).
10. U. C. Krieg, P. Walter, A. E. Johnson, *Proc. Natl. Acad. Sci. U.S.A.* **83**, 8604 (1986).
11. H. D. Bernstein *et al.*, *Nature* **340**, 482 (1989).
12. T. Connolly, R. Gilmore, *Cell* **57**, 599 (1989).
13. J. D. Miller, S. Tajima, L. Lauffer, P. Walter, *J. Cell Biol.* **128**, 273 (1995).
14. G. Bacher, H. Lütcke, B. Jungnickel, T. A. Rapoport, B. Dobberstein, *Nature* **381**, 248 (1996).
15. Materials and methods are available as supporting material on *Science* Online.
16. S. Hauser, G. Bacher, B. Dobberstein, H. Lütcke, *EMBO J.* **14**, 5485 (1995).
17. J. Luirink *et al.*, *Nature* **359**, 741 (1992).
18. M. R. Pool, B. Dobberstein, data not shown.
19. J. Walleczek, B. Redl, M. Stöffler-Meilicke, G. Stöffler, *J. Biol. Chem.* **264**, 4231 (1987).
20. N. Ban, P. Nissen, J. Hansen, P. B. Moore, T. A. Steitz, *Science* **289**, 905 (2000).
21. P. J. Rapiejko, R. Gilmore, *Cell* **89**, 703 (1997).
22. T. A. Fulga, I. Sinning, B. Dobberstein, M. R. Pool, *EMBO J.* **20**, 2338 (2001).
23. P. Nissen, J. Hansen, N. Ban, P. B. Moore, T. A. Steitz, *Science* **289**, 920 (2000).
24. C. M. T. Spahn *et al.*, *Cell* **107**, 373 (2001).
25. B. Jungnickel, T. A. Rapoport, *Cell* **82**, 261 (1995).
26. S. C. Ogg, P. Walter, *Cell* **81**, 1075 (1995).
27. Y. Lu *et al.*, *EMBO J.* **20**, 6724 (2001).
28. R. Beckmann *et al.*, *Science* **278**, 2123 (1997).
29. J. Menetret *et al.*, *Mol. Cell* **6**, 1219 (2000).
30. R. Beckmann *et al.*, *Cell* **107**, 361 (2001).
31. A. Neuhof, M. M. Rolls, B. Jungnickel, K.-U. Kalies, T. A. Rapoport, *Mol. Biol. Cell* **9**, 103 (1998).

32. We thank K. Meese for excellent technical assistance with antibody production, G. Bacher and members of the laboratory for insightful discussion, and C.-L. Owen for critical reading of the manuscript. This work was funded by an European Union Training and Mobility of Researchers (TMR) network grant (ERBFMRXCT-960035; B.D. and I.S.), Deutsche Forschungsgemeinschaft (DFG) Schwerpunkt Programm 312 (DO199/10-3; B.D.) SFB352/B17 (I.S.), SFB352/B1 (B.D.), and a Louis-Jeantet Fellowship (T.A.F.).

Supporting Online Material

www.sciencemag.org/cgi/content/full/297/5585/1345/DC1
Materials and Methods
Figs. S1 and S2
References and Notes

29 March 2002; accepted 9 July 2002